Lung involvement in patients with coronavirus disease-19 (COVID-19): a retrospective study based on quantitative CT findings

Nan Yu[1] · Cong Shen[2] · Yong Yu[1] · Minghai Dang[3] · Shubo Cai[4] · Youmin Guo[5]

Abstract

Purpose To explore lung involvement in patients with coronavirus disease-19 (COVID-19) using quantitative computed tomography (QCT).

Methods A total of 52 patients with COVID-19 who were admitted to three hospitals in China from January 23, 2020 to February 1, 2020 were retrospectively analyzed using QCT. The accuracy of QCT segmentation was assessed. The relationship between the time from symptom onset to initial CT and QCT parameters acquired on the initial CT were explored.

Results First, the ability of QCT to detect and segment lesions was investigated and it was unveiled that results of segmentation of the majority of cases (42/52) were satisfactory and for 8 out of 52 patients, the images depicted lesions with miss-segmentation; besides, 2 out of 52 cases had negative finding on chest CT achieved by both radiologists and QCT. QCT-related parameters showed to have a relationship with the time from symptom onset to initial CT. In the early-stage (0–3 days), the percentage of lung involvement was 4%, with a mean density of -462 ± 99 HU. The peak density of lesions appeared at the range of -500 to -700 HU on density histogram. In the intermediate-stage (4–6 days), the mean percentage of lung involvement noticeably increased compared with that in early stage (7%, $p < 0.05$). In late stage (7–14 days), the percentage of lung involvement decreased to 5%. The mean density of lesions was the highest (-430 ± 80), and heterogeneity density distribution showed a dual-peak on density histogram.

Conclusion COVID-19 can be promptly detected by QCT. In addition, the QCT-related parameters can highly facilitate assessment of pulmonary involvement.

Keywords Lung · Computed tomography · COVID-19

Introduction

The outbreak of coronavirus-19 (COVID-19) pneumonia emerged in Wuhan, the capital of Hubei Province in Central China, since December 2019. Thereafter, prevalence of COVID-19 has been reported in other provinces in mainland China and several other countries [1–6]. According previous reports [1, 7], the most common clinical symptom of COVID-19 is fever. In addition, other common symptoms include cough, sore throat, dyspnea, headache, and muscle fatigue [7, 8].

To date, several diagnostic methods for chest radiography, e.g. computed tomography (CT), have been reported [9, 10]. For instance, a prospective analysis reviewed chest CT scans of 21 symptomatic patients with 2019-nCoV, and they found mild or moderate progression of disease, as manifested by increasing extent and density of lung opacities according to findings of follow-up imaging [11]. Besides, interstitial lung abnormalities related to disease time course were also reported, and it was revealed that chest CT play a significant role in evaluating the progress of COVID-19 infection.

Quantitative CT (QCT) technique measures bone mineral density using a standard X-ray CT scanner with a calibration

✉ Youmin Guo
  cjr.guoyoumin@vip.163.com

1 Department of Radiology, Affiliated Hospital of Shaanxi University of Chinese Medicine, Xian Yang, China

2 Department of Radiology, Affiliated Hospital of Xi'an Jiaotong University, Xi'an, China

3 Department of Radiology, Number 9 Affiliated Hospital of Xi'an Jiaotong University, Xi'an, China

4 Department of Radiology, Xi'an Chest hospital, Xi'an, China

5 Department of Radiology, Affiliated Hospital of Xi'an Jiaotong University, Yanta west road 277#, Xi'an, China

standard to convert Hounsfield Units (HU) of the CT image to bone mineral density values. This method has been reported for the evaluation of a variety of interstitial lung abnormalities, such as vascular-embolic disorders, bronchiectasis, emphysema, pulmonary fibrosis, etc.

The present study quantitatively analyzed chest CT findings of 52 patients who were infected with COVID-19. The purpose of this study was to evaluate the accuracy of QCT in detecting and segmenting lesions, and explore the relationship between QCT-related indicators and development of the disease.

Patients and methods

Patients

Our institutional review board (IRB) waived written informed consent for this retrospective study. A total of 52 patients with COVID-19 who were admitted to 3 hospitals in Shaanxi province (China) were enrolled in this study. All the patients received chest CT. The diagnostic criterion was that real-time fluorescence polymerase chain reaction revealed positive detection of COVID-19 in throat swabs or lower respiratory tract.

CT protocol

CT scan was performed using three CT scanners, including UCT-760 scanner (Shanghai United Imaging Healthcare Co., Ltd., Shanghai, China), Discovery CT750 HD (GE Healthcare, Chicago, IL, USA), and Philips Brilliance Big Bore scanner (Philips Healthcare, Amsterdam, Netherlands). All scans were performed without intravenous contrast on patients who were placed in the supine position at the end inspiration phase. Images were reconstructed to encompass the entire lung field in a 512×512-pixel matrix using a standard algorithm at a 1-mm section thickness and a 1-mm interval.

QCT analysis

QCT was carried out on all CT scans. FACT-Digital lung TM software (DeXin, Xi'an, China) was used to perform fully automated three-dimensional CT quantitative measurements. The steps of segmentation were briefly undertaken as follows: (1) segmentation of the whole lung: a well-established thresholding operation was used to extract the lung volume. The threshold is determined based on intensity histogram analysis of the CT images; (2) segmentation of abnormal opacity: it was conducted by means of a 3D region-growing algorithm and a histogram-based thresholding technique; (3) bronchus and pulmonary vessels were segmented: a differential geometric approach was applied to automatically segment the vascular tree and airway tree. A "puzzle game" procedure acting as a "correction" operation for filtering false identifications was utilized; (4) quantitative evaluation of lesion's volume was conducted after segmentation. The quantitative parameters included the lung volume (LV), total lesion volume (TLV), and percentage of abnormal opacity volume (lesion%). The pixels in abnormal opacity were processed with histogram analysis including an illustration of pixel attenuation (CT numbers). Histogram analysis also allowed measurements of mean density (MD) and the proportion of pixels related to ground-glass opacity (GGO). The details of the algorithm used in the software have been reported in previous studies ([12–15]; see Fig. 1).

The results of segmentation were reviewed and verified by two radiologists independently. If the boundary of lesions was not segmented correctly with missed lesions, the lesions were manually segmented by radiologists, and percentage of lung involvement was re-calculated. In

Fig. 1 The steps of segmentation
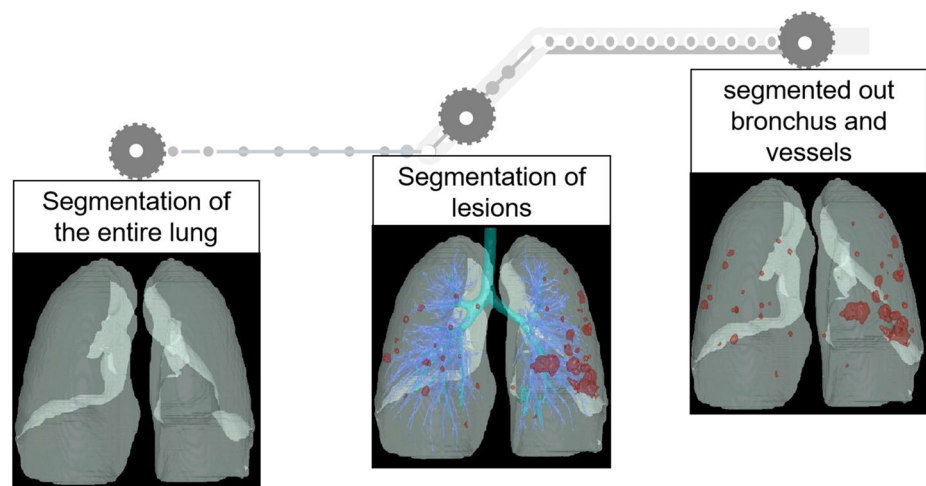
the case of disagreement, final results were determined by consensus and serviced as reference standards. The accuracy of segmentation by QCT was identified as follows: (1) the boundary of lesions was well segmented, without missed lesions; (2) the boundary of lesions was not segmented accurately, without missed lesions; (3) the boundary of lesions was not segmented correctly, with missed lesions.

Statistical analysis

All statistical analyses were undertaken using SPSS 17.0 software (IBM, Armonk, NY, USA). The independent-samples t test was used to analyze the parameters of the two groups, which were consistent with normal distribution and homogeneity of variance. Otherwise, the Mann–Whitney U test was employed. The normally distributed data were expressed as mean ± standard deviation (SD). Besides, the qualitative variables were presented as absolute numbers and percentages. $p < 0.05$ was considered statistically significant.

Results

Patients' clinical characteristics

A total of 52 patients were included in this study. The time from symptom onset to initial CT was 4.6 ± 2.9 days. According to the mentioned parameter, the patients were divided into three stage-based groups: early-stage group (1–3 days), intermediate-stage group (4–6 days), and late-stage group (7–14 days). The patients' clinical characteristics are summarized in Table 1. Common symptoms of infected patients were fever, sore throat, fatigue, cough and diarrhea. There were nine patients without fever, four patients with shortness of breath, and two patients with diarrhea (Table 1).

QCT results

Of 52 images, 42 were classified in level 1 (Fig. 2) and 8 were in level 2 (Fig. 3). No case was found in level 3. Two cases had negative findings on chest CT, who were both identified by radiologists and QCT. The time required to process one chest CT was 5 min.

Table 1 Patients' demographic and clinical characteristics

|	Time from symptom onset to initial CT			
	Patients $n = 52$	0–3 days $n = 21$	4–6 days $n = 18$	7–14 days $n = 13$
Gender (male)		13 (60)	8 (44)	9 (69)
Age (years)	45.3 ± 16.0	44.0 ± 17.8	47.0 ± 14.2	45.0 ± 16.4
Exposure				
Residency in Wuhan	41 (78)	14 (66)	14 (77)	13 (100)
Clustered cases	7 (13)	5 (24)	2 (11)	0 (0)
Close contact with COVID-19 patients	3 (6)	3 (14)	0 (0)	0 (0)
Unknown	1 (2)	0 (0)	1 (5)	0 (0)
Symptom				
No fever	9 (17)	5 (24)	4 (22)	0 (0)
Dyspnea	4 (8)	0 (0)	3 (17)	1 (8)
Diarrhea	2 (4)	0 (0)	2 (11)	0 (0)
Negative CT finding	2 (4)	2 (10)	0 (0)	0 (0)
QCT parameters				
LV	4206 ± 1060	4143 ± 1098	4004 ± 848	4589 ± 1233
TLV	204 ± 262	154 ± 177	$270 \pm 378*$	193 ± 169
Lesion%	5 ± 3	4 ± 4	$7 \pm 9*$	5 ± 4
MD	-446 ± 100	-462 ± 99	-439 ± 116	-430 ± 80
GGO%	20 ± 15	21 ± 16	20 ± 14	18 ± 15

LV lung volume, *TLV* total lesion volume, *Lesion*% the percentage of lung involvement, *MD* mean density, *GGO*% proportion of pixels related to ground-glass opacity (GGO)

$*p < 0.05$, compared with corresponding indexes during 0–3 days

Fig. 2 Chest CT findings of a 42-year-old male with COVID-19. **a** An axial CT image obtained from a 42-year-old male shows that multiple GGOs were segmented; **b** abnormal opacities were segmented; **c** three-dimensional volume-rendered reconstruction illustrates the distribution of the abnormal opacity
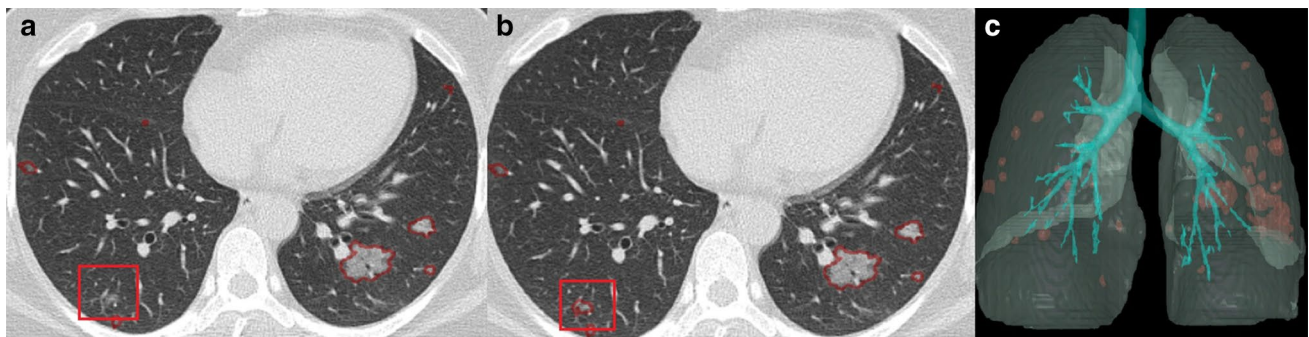
Fig. 3 Chest CT findings of a 38-year-old-male with COVID-19. The segmentation results of lesions in a 38-year-old patient indicated that, a small focal GGO was not initially detected (**a**), and the lesion was re-segmented manually (**b**). QCT results revealed that **c** the percentage of lung involvement increased from 1.63 to 1.64%
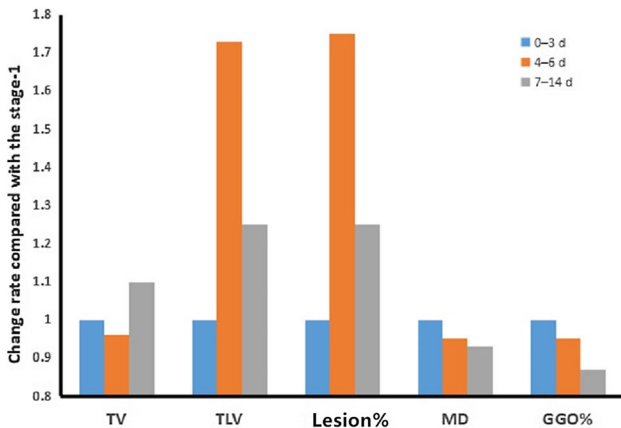
**Fig. 4** Frequency of QCT parameters compared with those in stage-1

QCT-related parameters were found to be correlated with symptom-onset time (Table 1, Fig. 4). The mean value of lesion was larger during 4–6 days (7%; range 0.4–36%) than that in 0–3 days (4%; range 0–18%), and that during 7–14 days (5%; range 0.3–17%). The value of LV was minimum in intermediate-stage group. During infection, MD of lesions increased from early stage to late stage. Density histogram also showed the characteristics of density distribution in each stage-based group. At early-stage (0–3 days), density histogram displayed a single peak that appeared in the range of − 500 to − 700 HU (Fig. 5a). At intermediate-stage (4–6 days), the peak of density moved to a higher range at − 400 to − 600 HU (Fig. 5b). At late-stage (7–14 days), density histogram distribution was more scattered at the range of − 800 to 100 HU (Fig. 5c). The proportion of pixels related to GGO decreased during the infection.

Discussion

In the present study, chest CT of 52 patients with COVID-19 was analyzed using QCT. In the analysis of all 52 images, the results of segmentation for the majority of cases (42/52) were satisfactory, and for 8 out of 52 patients, the images depicted lesions with miss-segmentation. After manual segmentation, we calculated the mean volume of missed lesions. The average volume (%) of missed lesions in the lung was
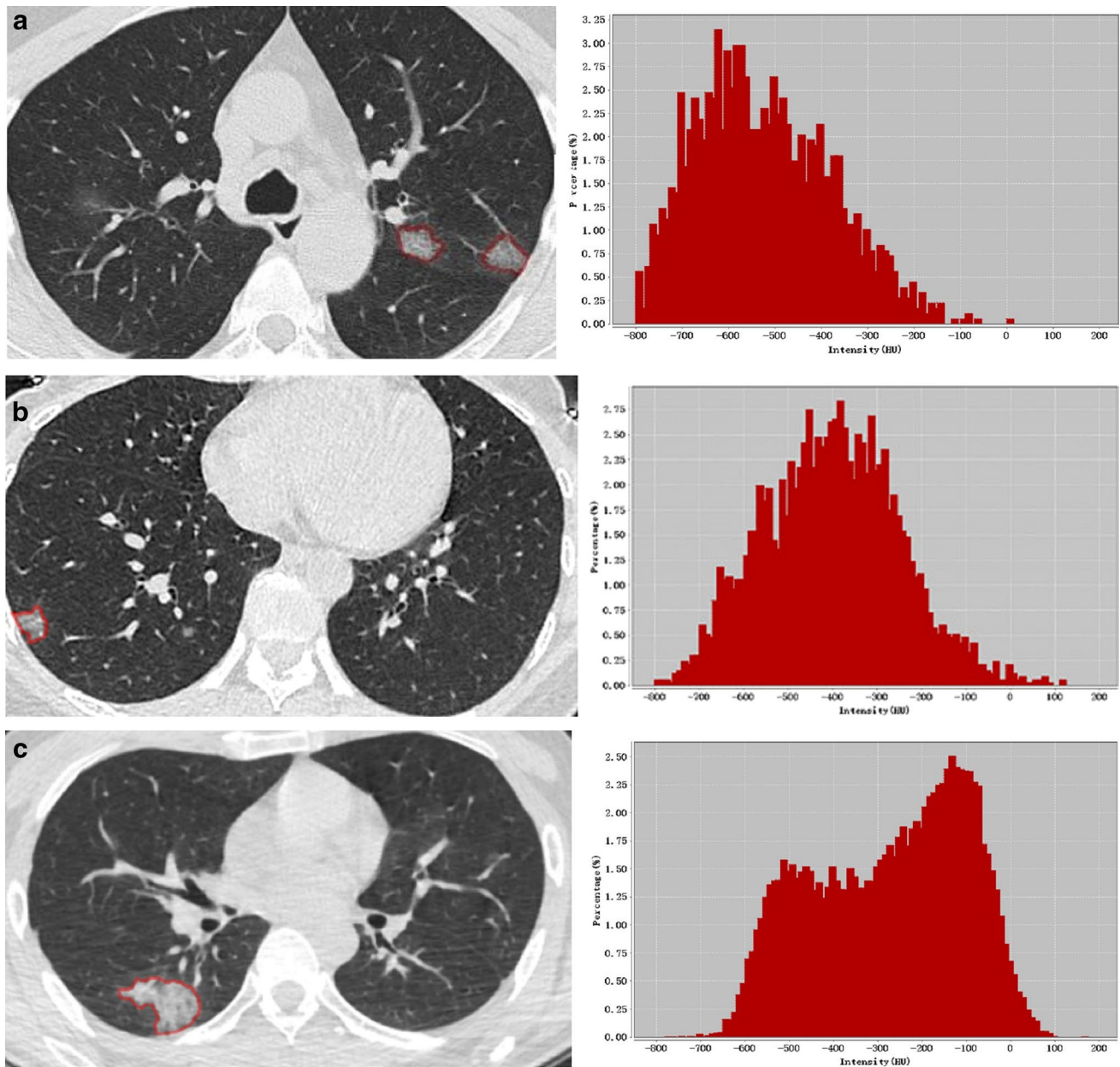
Fig. 5 Chest CT findings of patients with COVID-19. **a–c** The images show chest CT findings for three different patients, in which the values of time from symptom onset to initial CT were 2, 4, and 7 days, respectively. The density histogram shows a different pattern

0.01%. Compared with the percentage of lung involvement, the impact of miss-segmentation was insignificant. Lesions with miss-segmentation were observed in the following situations: (1) the lesions were adjacent to the blood vessels, and the vessels were wrongly as lesions; (2) the lesions were adjacent to the heart, and the heart beat artifacts affected the segmentation of the lesions; (3) the lesions were extremely small for segmentation (Fig. 3).

QCT provides quantitative parameters to assess both extent and density of abnormal opacity. The range of percentage of lung involvement was herein 0–36%. The density of the lesion was assessed by CT value histogram. The CT patterns of GGO, GGO with crazy-paving pattern and consolidation exhibited to have different density characteristics and overall distribution characteristics (Fig. 4). According to the distribution of CT value histogram, we not only observed the average density, but also the density distribution below − 450 HU to describe GGO.

In addition, quantitative parameters of QCT are helpful to describe the imaging changes in the course of disease. QCT parameters are related to the symptom-onset time. In the current research, the mean density increased with the

time course of infection, which was consistent with results of a previous study [9]. GGO with homogeneous density was found in early-stage group, with increased crazy-paving pattern in intermediate-stage group, and gradual consolidation in late-stage group. The evaluation of the extent of lesion is highly essential for judgment of disease progress. Additionally, in the present research, QCT was used to segment and extract the features of lesions, making the judgment of the extent of lesions more objectively and accurately.

The QCT could herein automatically segment and identify lung volume, bronchus, small pulmonary vessels, and abnormal opacity. It is a three-dimensional (3D) non-projection technique possessing a number of advantages to other densitometry techniques including high accuracy in segmentation, and easiness of operation. This approach was reported in our previous publication, and proven ability to segment accurately.

There are several limitations in the current study. The influence of reconstruction layer thickness on segmentation results was not assessed. Furthermore, there might a selection bias that is particularly related to the pattern of diagnosing patients with mild and moderate degree of disease, while lack of patients with severe-degree of disease was tangible.

In summary, COVID-19 can be swiftly detected by QCT. QCT can provide quantitative indexes to describe both extent and density of abnormal opacity. In addition, the changes of QCT-related parameters can provide reference data for evaluating the progress of disease.

Compliance with ethical standards

Conflict of interest The authors have no conflict of interest.

References

1. Huang C, Wang Y, Li X, Ren L, Zhao J, Hu Y, Zhang L, Fan G, Xu J, Gu X, Cheng Z, Yu T, Xia J, Wei Y, Wu W, Xie X, Yin W, Li H, Liu M, Xiao Y, Gao H, Guo L, Xie J, Wang G, Jiang R, Gao Z, Jin Q, Wang J, Cao B. Clinical features of patients infected with 2019 novel coronavirus in Wuhan, China. Lancet. 2020. https://doi.org/10.1016/S0140-6736(20)30183-5.
2. Li Q, Guan X, Wu P, Wang X, Zhou L, Tong Y, Ren R, Leung KSM, Lau EHY, Wong JY, Xing X, Xiang N, Wu Y, Li C, Chen Q, Li D, Liu T, Zhao J, Li M, Tu W, Chen C, Jin L, Yang R, Wang Q, Zhou S, Wang R, Liu H, Luo Y, Liu Y, Shao G, Li H, Tao Z, Yang Y, Deng Z, Liu B, Ma Z, Zhang Y, Shi G, Lam TTY, Wu JTK, Gao GF, Cowling BJ, Yang B, Leung GM, Feng Z. Early transmission dynamics in Wuhan, China, of novel coronavirus-infected pneumonia. N Engl J Med. 2020. https://doi.org/10.1056/NEJMoa2001316.
3. Zhu N, Zhang D, Wang W, Li X, Yang B, Song J, Zhao X, Huang B, Shi W, Lu R, Niu P, Zhan F, Ma X, Wang D, Xu W, Wu G, Gao GF, Tan W, China Novel Coronavirus I, Research T. A novel coronavirus from patients with pneumonia in China, 2019. N Engl J Med. 2020. https://doi.org/10.1056/NEJMoa2001017.
4. World Health Organization. Novel coronavirus (2019-nCoV). Situation report 22. Geneva, Switzerland: World Health Organization. 2020. https://wwwwhoint/docs/defaultsource/coronaviruse/situation-reports/20200211-sitrep-22-ncovpdf?sfvrsn=fb6d49b1_2. Accessed 11 Feb 2020.
5. World Health Organization. Clinical management of severe acute respiratory infection when novelcoronavirus (nCoV) infection is suspected: interim guidance. https://wwwwhoint/docs/defaultsource/coronaviruse/clinical-management-of-novel-covpdf?sfvrsn=bc7da517_2. Accessed 12 Jan 2020.
6. Wang D, Hu B, Hu C, Zhu F, Liu X, Zhang J, Wang B, Xiang H, Cheng Z, Xiong Y, Zhao Y, Li Y, Wang X, Peng Z. Clinical Characteristics of 138 Hospitalized Patients With 2019 Novel Coronavirus-Infected Pneumonia in Wuhan, China. JAMA. 2020. https://doi.org/10.1001/jama.2020.1585.
7. Wang W, Tang J, Wei F. Updated understanding of the outbreak of 2019 novel coronavirus (2019-nCoV) in Wuhan, China. J Med Virol. 2020. https://doi.org/10.1002/jmv.25689 **(Epub ahead of print)**.
8. Xie X, Zhong Z, Zhao W, Zheng C, Wang F, Liu J. for typical 2019-nCoV pneumonia: relationship to negative RT-PCR testing. Radiology. 2020. https://doi.org/10.1148/radiol.2020200343 **(Epub ahead of print)**.
9. Pan F, Ye T, Sun P, et al. Time course of lung changes on chest CT during recovery from 2019 novel coronavirus (COVID-19) pneumonia. Radiology. 2020. https://doi.org/10.1148/radiol.2020200370 **(Epub ahead of print)**.
10. Chung M, Mernheim A, Mei X, et al. 2019 Novel coronavirus (2019-nCoV). Radiology. 2020. https://doi.org/10.1148/radiol.2020200230 **(Epub ahead of print)**.
11. Pu J, Fuhrman C, Good WF, et al. A differential geometric approach to automated segmentation of human airway tree. IEEE Trans Med Imaging. 2011;30:266–78.
12. Pu J, Roos J, Yi CA, et al. Adaptive border marching algorithm: automatic lung segmentation on chest CT images. Comput Med Imaging Graph. 2008;32:452–62.
13. Pu J, Leader JK, Zheng B, et al. A computational geometry approach to automated pulmonary fissure segmentation in CT examinations. IEEE Tran Med Imaging. 2009;28:710–9.
14. Pu J, Zheng B, Leader JK, Gur D, et al. Pulmonary lobe segmentation in CT examinations using implicit surface fitting. IEEE Trans Med Imaging. 2009;28:1986–96.
15. Bernheim A, Mei X, Huang M, Yang Y, Fayad ZA, et al. Chest CT findings in coronavirus disease-19 (COVID-19): relationship to duration of infection. Radiology. 2020. https://doi.org/10.1148/radiol.2020200230 **(Epub ahead of print)**.

Publisher's Note Springer Nature remains neutral with regard to jurisdictional claims in published maps and institutional affiliations.